# Myorcadial Infarction Classification with 15 Lead Electrocardiogram (ECG) Signal using Hybrid Convolutional Neural Network (CNN) and Bidirectional Long Short-Term Memory (BILSTM)

2023 Eighth International Conference on Informatics and Computing (ICIC) | 979-8-3503-4260-4/23/$31.00 ©2023 IEEE | DOI: 10.1109/ICIC60109.2023.10381905

Ahmad Haidar Mirza
*Faculty Of Engineering*
*Universitas Sriwijaya*
*Faculty Of Computer Science*
*Universitas Bina Darma*
Palembang, Indonesia
haidar.mirza06@gmail.com

Siti Nurmaini
*Intelligent System Research Group*
*Faculty of Computer Science,*
*University of Sriwijaya*
Palembang, Indonesia
siti_nurmaini@unsri.ac.id

Radiyati Umi Partan
*Faculty of Medicine,*
*Universitas Sriwijaya*
Palembang, Indonesia
radiyati.u.p@fk.unsri.ac.id

Muhammad Izman Herdiansyah
*Faculty Of Computer Science*
*Universitas Bina Darma*
Palembang, Indonesia
m.herdiansyah@binadarma.ac.id

***Abstract*—More than three branches of death due to cardiovascular disease. Myocardial infarction (MI) is one of the most dangerous forms of coronary heart disease, with the highest mortality rate among other types of coronary heart disease. MI is caused by reduced oxygen demand in heart muscle tissue when oxygen is pumped throughout the body. To detect MI, experts can use ECG signals. ECG is a tool that can be used to record the activity of biological signals formed due to the electrical activity of the heart. Various studies have been conducted using deep learning to help detect and predict MI. This research proposes a hybrid model of CNN-LSTM and CNN-BILSTM model techniques to predict MI. The MI dataset from the Physiobank (PTB) ECG database consisting of 52 normal subjects and 148 patients was used for training models. The proposed deep learning model uses automatic feature extraction. This study suggests a simple deep learning architecture with automatic feature extraction to learn from data. Evaluation of model performance resulted in an average accuracy of 98.80% for the CNN-LSTM model and 99.90% for the CNN-BILSTM model.**

***Keywords—myocardial infarction, CNN, LSTM, BILSTM, deep learning***

## I. INTRODUCTION

According to a WHO study in 2019, Ischemic Heart Disease (IHD) is the world's leading cause of death at 16% and has steadily risen to 8.9 million in the last two decades [1]. Cardiovascular disease (CVD) was expected to be the leading cause of death in develop country and developing country by 2020 [2]. In Indonesia, the number of people suffering from coronary heart disease is 883,447 or 0.5%. According to Riset Kesehatan Dasar (Riskesdas) in 2018, heart and blood vessel disease is increasing every year. It is estimated that around 2,784,064 people in Indonesia suffer from heart disease, which is equivalent to 15 out of every 1000 people. Myocardial Infarction (MI) is the most dangerous form of coronary heart disease with the highest death rate compared to other types of coronary heart disease [3]. Lack of oxygen supply to heart muscle tissue can cause MI. When the activity of the heart muscle increases, the need for oxygen needed by the body also increases [4]. Heart attacks, also known as MI, often occur in patients who have a history of heart disease. The main clinical features of MI are heart failure, angina pectoris, and arrhythmias [5]. Hypertension, history of cardiovascular disease, and diabetes are the main factors that can predict the risk of MI [6]. To be able to know and detect MI, experts use ECG signals [7].

An ECG is a tool that places electrodes at certain points on the body to record biological signal activity from the heart's electrical activity [8]. The ECG signal has a certain form which can be used as a reference for determining heart health conditions [9]. Patients who experience MI symptoms are observed with ECG signal changes in ST interval length, ST elevation and changes in T wave shape [10]. In contrast to MI patients, in normal patients the five waves (P, QRS, and T) have no morphology [11]. Observation will be difficult due to variations in the morphology of the ECG signal in each different patient with different physical conditions [12].

The lead ECG describes electrical activity specifically based on observations that make it possible to differentiate various types of MI attacks in the heart based on the location of the infarction in the myocardium [13]. For example, the combination of leads V1, V2, V3, and V4 indicates an anterior MI (AMI), while the combination of leads II, III, and aVF may indicate an inferior MI. However, 12-lead ECG has difficulty identifying the location of posterior myocardial infarction [14], [15]. A study by Gupta et al [16] measured the contribution to the 15-lead ECG signal and identified leads V5, V6, Vx, Vz, and II, which were then quantified in pairs using the five main channels. The results of this study are that lead V6 and lead Vz provide the best performance of the five leads. Fu et al [17] used a systematic approach to select the most important leads in the process of diagnosis and localization of intra-patient and inter-patient MI in a regional setting, although it only aims to help the proposed deep learning method for effective.

In the last few decades, research related to MI with deep learning approaches has shown several advantages compared to machine learning approaches[1]. Several deep learning algorithms that have been implemented for MI classification

and detection include CNN [18], Recurrent Neural Network (RNN) and Long Short-Term Memory (LSTM) as proposals for binary classification of MI patients and normal patients [19]. Among these algorithms, CNN is known for feature recognition. The application of one-dimensional (1D) CNNs in the medical field has grown rapidly, especially in the fields of physiology and radiology where researchers treat ECG signals like one-dimensional (1D) images. They applied it in the diagnosis of arrhythmias and MI through single individual signals [20]. 1D CNN is also used to detect other heart diseases such as Atrial Fibrillation (AF) [21]. This research focuses on the CNN algorithm approach to classify all MI classes on 15-lead ECG signals. This is because 12-lead ECG signals have difficulty in localizing posterior MI [14], [15]. The development of a simple 1D CNN architecture model is a consideration to reduce computing time in addition to getting better performance. Apart from CNN which is well known for its ability in feature recognition, LSTM and BILSTM will help process temporal features in ECG data. This motivates researchers to consider using a CNN architecture combined with LSTM and BILSTM in this research. Based on the description above, this research can make the following contributions:

- Proposed model with better simple architecture with CNN and LSTM/BILSTM.
- Development of the CNN-LSTM and CNN-BILSTM models to classify 10 MI classes and one Normal class (Healthy class) in 15-lead ECG signals.

This paper is organized in the following order. Section 2 explains the materials and methods used. Section 3 describes result dan analysis model. Section 4 discusses model evaluation. Section 5 provides the conclusions of this study.

## II. Material and Method

In this section, the model sequencing process is discussed. The flowchart is as shown in the following figure :

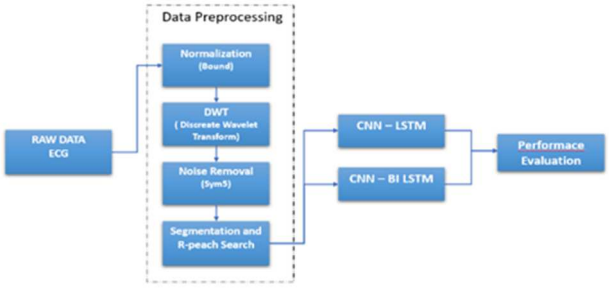


Fig. 1. Flowchat of the proposed Model

### A. Data Preprocessing

The raw data used in this study were sourced from the non-commercial Physiobank (PTB) open access ECG database [22]. The entire PTB database contains 549 records from 290 subjects. Each signal is digitized with a resolution of 16 bits in the range of ± 16.384 mV at 1000 samples per second. The dataset we use in this study is Myocardial Infarction (MI) data which consists of ECG recordings from 52 normal patients and 148 MI patients. The number of leads used is 15 multi-lead ECG signals with 12 standard leads and 3 Frank leads with eleven class groupings, namely anterior (A), anterolateral (AL), anteroseptal (AS), inferior (I), inferolateral (IL), inferior posterior (IP). ), infero-posterolateral (IPL), lateral (L), posterior (P) and posterolateral (PL) and normal/healthy.

Data Preprocessing stage consists of four main stages, namely: normalization, Discrete Wavelet Transform (DWT), noise removal and R-peak search and finally the segmentation stage. Raw ECG signal recordings require normalization because features have different ranges. The Normalized Bound function is a function used to normalize a signal which only changes the signal amplitude scale within a certain range without changing the signal morphology. This process will reduce computing time.

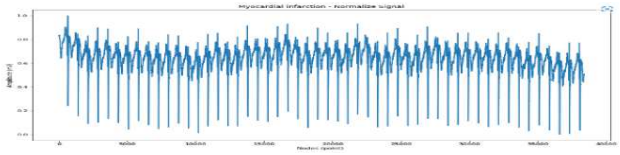

Fig. 2. Normalized Sample

After normalization, ECG signal analysis is carried out to detect noise with Discrete Wavelet Transform (DWT). DWT is used to analyze signals that are localized in time and frequency. To eliminate ECG signal interference (noise removal) after the normalization process, we use Sym5 as a mother wavelet for a better ECG signal denoising process [21].

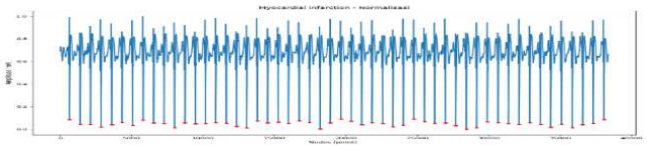

Fig. 3. Noise Removal Sample

The signal that is clean of noise is then segmented and R-peak detection is carried out (looking for the highest positive point of the QRS point in the ECG signal cycle). Segmentation is a step to differentiate the waveforms of each beat and the next heartbeat [23] The frequency of the ECG signal with a duration of t1 is 0.25 seconds before the R-peak and a duration of t2 is 0.45 seconds after the R-peak. The signal length is 0.7 seconds with an average of between 60 – 80 beats per minute. A total of 0.7 seconds contains 700 nodes, which are divided into two intervals t1 of 250 nodes and t2 of 450 nodes [18]. The segmentation results can be seen from the distribution curve for each class below (figure 4).

Different characteristics are shown by each ECG signal from each lead. It represents vector information from sensor locations placed at different geographic locations of the chest. For example, the ECG signal waveform in lead V2 for normal class and 10 MI class.

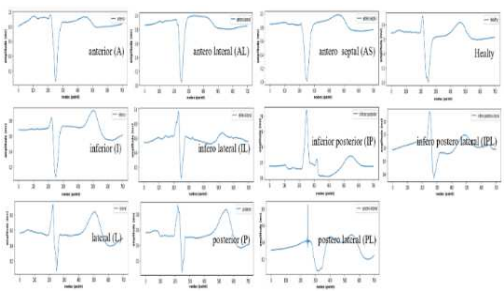


Fig. 4. 10 class MI and Normal class

The distribution of each number of pulses of training data for each class and lead is presented in Figures 5 and 6.

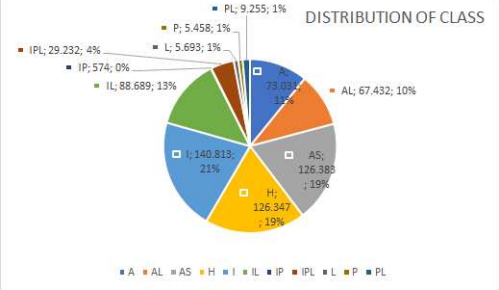


Fig. 5. Distribution of data training on each class

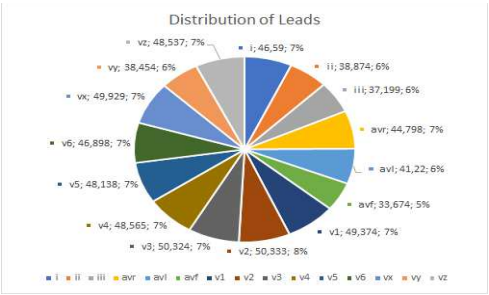


Fig. 6. Distribution of data training on each leads

## B. CNN - LSTM

After the ECG signal is segmented, the next step is to classify it with the CNN – LSTM architecture. CNN is a popular feature extraction and classification method of time-series data. CNN was originally introduced by LeCun in the early 90's [24]. CNN is similar to multilayer perceptron (MLP). This special structure allows CNNs to have translation and rotation invariants due to the model architecture [25]. In general, CNN consists of one or more convolutional layers, the fully connected layer at the top, including the weights and the pooling layer [26]. he CNN classification method used is CNN 1D. The ECG feature map is built using 2 convolution layers. In the first stage, a signal with a length of 700 nodes will be filtered by 64 nodes with a 5x1 kernel with the ReLu activation function. After non-linear processing, a feature map will be produced from the convolution process which will function as new input for the next process. The ReLu function is a non-linear function that is used to prevent grandiens from occurring in the training phase. Then the Maxpooling and Dropout layers with a rate value of 0.2 are added to prevent over-fitting and speed up the learning process. In second convolution layer with 64 filters and 3x1 kernel with Relu activation function. The results of the CNN will be input with a total of 64 nodes for the LSTM layer. There are three types of gates in LSTM, forget gates, input gates, and output gates. With these three gates, relevant information will be passed on through cell status to make predictions [27]. After that we added the Flatten layer. This layer is useful for converting multidimensional arrays into vectors to reshape feature maps which will then become input for the fully connected layer. The next layer adds a batch_normalization layer. Dense (Fully Connected Layer) 64 features with ReLu function. This Dense layer functions to classify according to the class in the output. Dense is a Neural Network model that has one input and has an output that corresponds to the number of classes to be classified/predicted. After that, add the Dropout layer. The last layer is the Dense layer with the Softmax activation function. From the experimental results, a simple CNN-LSTM architecture is obtained which consists of 9 layers with detailed parameters as shown in table 1.

TABLE I. DETAIL PARAMETER IN THE CNN-LSTM MODEL

| No | Layer | Output Shape | Parameter |
|---|---|---|---|
| 1 | conv1d (Conv1D) | (None, 696, 64) | 384 |
| 2 | max_pooling1d_1 (MaxPoolingID) | (None, 348, 64) | 0 |
| 3 | dropout (Dropout) | (None, 348, 64) | 0 |
| 4 | conv1d_1 (Conv1D) | (None, 346, 64) | 12352 |
| 5 | lstm (LSTM) | (None, 346, 64) | 33024 |
| 6 | flatten (Flatten) | (None, 22144) | 0 |
| 7 | dense (Dense) | (None, 64) | 1417280 |
| 8 | dropout_1 (Dropout) | (None, 64) | 0 |
| 9 | dense_1 (Dense) | (None, 11) | 715 |

Total params: 1463755 (5.58 MB)
Trainable params: 1463755 (5.58 MB)
Non-trainable params: 0 (0.00 Byte)

## C. CNN - BILSTM

The second model proposed is a model with a CNN architecture mixed with two-way LSTM (BILSTM). BILSTM is an LSTM that is used to capture two-way information by adding one LSTM layer to capture backflow information from an input sequence at each time interval. The input sequence is trained with a normal LSTM and another with a reverse copy LSTM of the input sequence [27]. Both will produce a final output which is combined to form the final vector. BILSTM CNN model architecture consists of 2 layers of CNN 64 nodes. The kernel is fixed at 7x1 for the first layer and 5x1 for the second layer. The first layer is followed by Maxpooling after the convolution layer. Data is forwarded through the BILSTM layer carrying 64 input nodes. After that, Global Maxpooling changes the data size according to what is needed to meet the dense layer size requirements. Dense with the Softmax activation function classifies data into 11 classes consisting of 10 MI classes and normal class. The proposed CNN-BILSTM model consists of 10 layers with details shown in table 2.

TABLE II. DETAIL PARAMETER IN THE CNN-BILSTM MODEL

| No | Layer | Output Shape | Parameter |
|---|---|---|---|
| 1 | conv1d (Conv1D) | (None, 696, 64) | 512 |
| 2 | max_pooling1d_1(MaxPooling ID) | (None, 347, 64) | 0 |
| 3 | dropout (Dropout) | (None, 347, 64) | 0 |
| 4 | conv1d_1 (Conv1D) | (None, 343, 64) | 20544 |
| 5 | bidirectional(Bidirectional) | (None, 346, 128) | 66048 |
| 6 | flatten (Flatten) | (None, 43904) | 0 |
| 7 | batch_normalization (Bach Normalization) | (None, 43904) | 175616 |
| 8 | dense (Dense) | (None, 64) | 2809920 |
| 9 | dropout_1 (Dropout) | (None, 64) | 0 |
| 10 | dense_1 (Dense) | (None, 11) | 715 |

Total params: 3073355 (11.72 MB)
Trainable params: 2985547 (11.39 MB)
Non-trainable params: 87808 (343.00 KB)

# III. RESULT AND ANALYSIS

After the CNN-LSTM model and CNN BILSTM model are built, each model will be compiled and configured to train data. Both models were trained by applying the categorical_crossentropy loss function, using the adam

optimizer with a learning rate (lr) of 0.001 and an accuracy model matrix. The next step is to train the model using the fit method. The fit method will accept arguments in the form of the input dataset to be trained, the output dataset to be trained and the number of epochs. Epochs is the number of cycles to train the entire dataset into several batches. The argument value for the epochs used in this code is 30 so it can be concluded that in order to carry out a complete training process, training is carried out 30 times for the entire dataset. The data is divided into the ratio of training data, validation data and testing data of 70:15:15 with training and validation data of 672,907 and testing data of 100,937. The following table 3 shows the results of performance measurements of the accuracy matrix of the CNN-LSTM (column 1) and CNN-BILSTM (column 2) models with 30 epochs on the 15 lead ECG test.

TABLE III. THE ACCURACY OF THE TRAINED CNN-LSTM/BILSTM MODEL ON THE TEST DATA

| LEAD | Traning Acc | | Validation Acc | | Testing Acc | |
|---|---|---|---|---|---|---|
| | *(1)* | *(2)* | *(1)* | *(2)* | *(1)* | *(2)* |
| I | 99,09% | 98,77% | 98,54% | 82,14% | 98,79% | 81.73% |
| II | 99,15% | 99,13% | 99,73% | 98,46% | 99,51% | 98,18% |
| III | 99,19% | 98,11% | 94,70% | 98,56% | 94,54% | 98,61% |
| aVR | 96,02% | 96,54% | 92,26% | 80.07% | 91,15% | 79,75% |
| aVL | 94,76% | 95,27% | 98,79% | 98,45% | 98,91% | 98,58% |
| aVF | 96,09% | 92,89% | 97,44% | 95,11% | 97,22% | 95,35% |
| V1 | 99,09% | 96,70% | 92.13% | 88,67% | 92,67% | 88,66% |
| V2 | 99,13% | 97,34% | 88,01% | 89,22% | 88,21% | 88,71% |
| V3 | 98,34% | 95,52% | 80,14% | 96,68% | 80,92% | 96,61% |
| V4 | 98,67% | 99,51% | 95,26% | 99,55% | 94,48% | 99,45% |
| V5 | 98,96% | 99,38% | 98,35% | 97,94% | 98,26% | 98,03% |
| V6 | 99,16% | 95,95% | 98,52% | 86,24% | 98,76% | 85,95% |
| Vx | 99,51% | 98,47% | 93,79% | 98,70% | 94,34% | 98,66% |
| I | 93,15% | 77,75% | 91,38% | 78,97% | 92,01% | 79,77% |
| II | 99,05% | 94,72% | 82,31% | 97,38% | 81,39% | 97,67% |
| AVG | 97,96% | 95,74% | 93,52% | 93,29% | 93,41% | 93,14% |

From measuring the accuracy matrix with 30 epochs on the CNN-LSTM model (Table 3), the best testing accuracy results were obtained in lead II with an testing accuracy value of 99.51%. The average accuracy value which includes training, validation and testing for the 15 leads for the entire CNN-LSTM model is 97.74%, 93.52% and 93.41%.

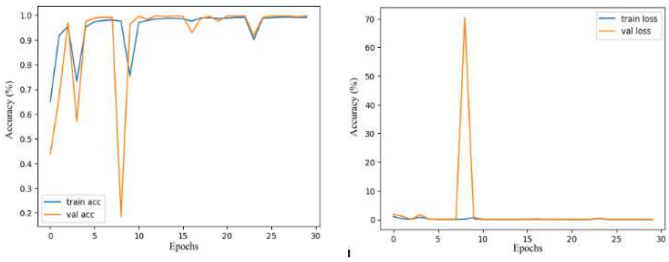


Fig. 7. Grafic Training and Validation (Accuracy and Loss) lead II

Measurements using the CNN-BILSTM model resulted in the best accuracy on lead v4 with accuracy testing results of 99.45% with average training, validation and testing accuracy testing values for 15 ECG leads of 95.74%, 93.29% and 93.14%. Following are the detailed Training and Validation (Accuracy and Loss) graphs for both models. The prospect lead II for CNN-LSTM and lead V4 for CNN-BILSTM are shown in the following image:

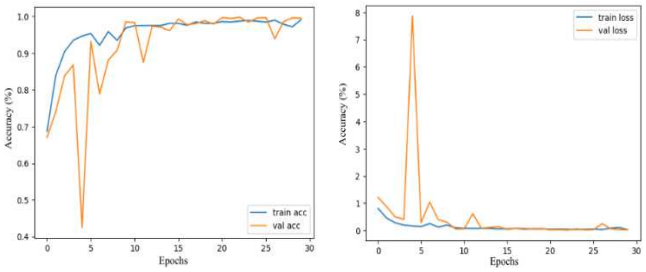


Fig. 8. Grafic Training and Validation (Accuracy and Loss) lead V4

## IV. EVALUATION PERFORMANCE

To measure the performance of the two proposed models, model performance is measured based on accuracy, precision, sensitivity and F1 score [27]. The formula for each measurement matrix is as follows:

$$\text{Accuracy (Acc)} = (TP + TN)/(TP + FP + FN + TN) \quad (1)$$
$$\text{Sensitivity (Sens)} = TP/(TP + FN) \quad (2)$$
$$\text{Specificity (Spe)} = TN/(TN+FP) \quad (3)$$
$$\text{Precision (Pre)} = TP/(TP + FP) \quad (4)$$
$$\text{F1-score} = 2 \times (Pre \times Sens) / (Pre + Sens) \quad (5)$$

True Positive (TP) is calculated from the number of positive classes correctly predicted by the model. True negative (TN) is calculated from the number of negative classes that the model predicts correctly. False positives (FP) are obtained from the number of positive classes that are incorrectly predicted and false negatives (FN) indicate the number of negative classes that are incorrectly predicted by the model.

Performance results of the proposed (in Table 4), CNN-LSTM architecture on 15 lead ECG with matrix accuracy, sensitivity, specificity, precision and f1-score with average values of 98.80%, 94.53%, 99.30%, 95.38% and 94.45%. Meanwhile, for the CNN-BILSTM architecture (in Table 5), performance matrices for accuracy, sensitivity, specificity, precision and f1-score were obtained with average values of 98.62%, 91.30%, 99.19%, 94.89% and 92.14%. The best leads for the CNN-LSTM and CNN-BILSTM architectures are lead II and lead V4 with average accuracy values of 99.93% and 99.90%.

TABLE IV. PERFORMANCE RESULT (%) 15 LEAD ECG ON THE PROPOSED CNN-LSTM ARSITECTURE

| Lead | ACC (%) | SEN (%) | SPE (%) | PRE (%) | F1-Score (%) |
|---|---|---|---|---|---|
| I | 99,78 | 98,03 | 99,87 | 99,08 | 98,53 |
| II | 99,93 | 99,42 | 99,96 | 99,74 | 99,58 |
| III | 99,01 | 94,95 | 99,42 | 96,53 | 95,49 |
| aVR | 98,41 | 86,69 | 99,06 | 94,88 | 89,43 |
| aVL | 99,80 | 98,68 | 99,88 | 99,08 | 98,87 |
| aVF | 99,49 | 97,75 | 99,70 | 98,29 | 97,99 |
| V1 | 98,67 | 93,17 | 99,18 | 96,43 | 94,54 |
| V2 | 97,86 | 92,63 | 98,75 | 86,16 | 87,69 |
| V3 | 96,53 | 88,07 | 97,99 | 90,48 | 87,85 |
| V4 | 99,00 | 96,23 | 99,40 | 96,73 | 96,36 |
| V5 | 99,68 | 98,38 | 99,81 | 98,04 | 97,99 |
| V6 | 99,77 | 98,43 | 99,87 | 99,13 | 98,73 |
| Vx | 98,97 | 97,00 | 99,41 | 92,51 | 94,26 |
| Vy | 98,55 | 91,43 | 99,16 | 94,23 | 91,89 |
| Vz | 96,62 | 87,06 | 97,99 | 89,44 | 87,48 |
| AVG | 98,80 | 94,53 | 99,30 | 95,38 | 94,45 |

TABLE V. PERFORMANCE RESULT (%) 15 LEAD ECG ON THE PROPOSED CNN-BILSTM ARSITECTURE

| Lead | ACC (%) | SEN (%) | SPE (%) | PRE (%) | F1-Score (%) |
|---|---|---|---|---|---|
| I | 96,68 | 84,43 | 98,05 | 87,80 | 84,61 |
| II | 99,67 | 97,91 | 99,80 | 98,86 | 98,36 |
| III | 99,75 | 98,92 | 99,85 | 98,60 | 98,75 |
| aVR | 96,32 | 80,49 | 97,80 | 89,08 | 73,08 |
| aVL | 99,74 | 98,77 | 99,85 | 98,76 | 98,76 |
| aVF | 99,16 | 96,93 | 99,52 | 96,37 | 96,59 |
| V1 | 97,94 | 75,70 | 98,82 | 92,06 | 86,28 |
| V2 | 97,95 | 89,84 | 98,81 | 93,05 | 90,44 |
| V3 | 99,38 | 98,28 | 99,64 | 98,05 | 98,08 |
| V4 | 99,90 | 99,59 | 99,94 | 99,60 | 99,60 |
| V5 | 99,64 | 96,42 | 99,78 | 98,86 | 97,55 |
| V6 | 97,45 | 80,28 | 98,50 | 85,45 | 80,72 |
| Vx | 99,76 | 97,54 | 99,86 | 99,01 | 98,18 |
| Vy | 96,32 | 76,42 | 97,86 | 89,42 | 82,95 |
| Vz | 99,58 | 97,99 | 99,75 | 98,33 | 98,13 |
| AVG | 98,62 | 91,30 | 99,19 | 94,89 | 92,14 |

Table 6 and table 7 explain the results of performance measurements on 10 MI classes and normal classes on the proposed CNN-LSTM and CNN-BILSTM architectural models.

TABLE VI. PERFORMANCE MATRIX (%) 10 MI CLASS AND NORMAL CLASS ON THE PROPOSED CNN-LSTM ARCHITECTURE

| Class | Performance Matrix | | | | |
|---|---|---|---|---|---|
| | *Accuracy* | *Sensitivity* | *Specificity* | *Precision* | *F1-score* |
| A | 98,07 | 92,54 | 98,75 | 91,51 | 91,29 |
| AL | 98,31 | 92,78 | 98,96 | 91,89 | 92,00 |
| AS | 97,83 | 92,77 | 99,01 | 95,78 | 94,09 |
| H | 97,88 | 93,47 | 98,87 | 95,86 | 94,20 |
| I | 97,33 | 92,52 | 98,60 | 94,76 | 93,09 |
| IL | 98,06 | 96,59 | 98,29 | 92,58 | 93,88 |
| IP | 99,93 | 98,44 | 100,00 | 97,78 | 97,82 |
| IPL | 99,66 | 91,62 | 99,89 | 97,37 | 93,92 |
| L | 99,89 | 94,68 | 99,93 | 95,83 | 94,03 |
| P | 99,94 | 96,19 | 99,98 | 97,73 | 96,47 |
| PL | 99,95 | 98,22 | 99,98 | 98,12 | 98,10 |
| AVG | 98,80 | 94,53 | 99,30 | 95,38 | 94,45 |

TABLE VII. PERFORMANCE MATRIX (%) 10 MI CLASS AND NORMAL CLASS ON THE PROPOSED CNN-BILSTM ARCHITECTURE

| Class | Performance Matrix | | | | |
|---|---|---|---|---|---|
| | *Accuracy* | *Sensitivity* | *Specificity* | *Precision* | *F1-Score* |
| A | 97,85 | 94,80 | 98,22 | 88,41 | 91,01 |
| AL | 98,38 | 91,10 | 99,17 | 92,98 | 91,58 |
| AS | 97,50 | 92,64 | 98,64 | 94,47 | 93,29 |
| H | 97,91 | 95,83 | 98,39 | 93,83 | 94,67 |
| I | 97,00 | 88,09 | 99,35 | 97,17 | 91,97 |
| IL | 97,28 | 95,32 | 97,56 | 87,71 | 90,74 |
| IP | 99,68 | 82,64 | 99,99 | 98,32 | 94,16 |
| IPL | 99,60 | 92,48 | 99,85 | 95,01 | 89,36 |
| L | 99,90 | 91,64 | 99,97 | 99,42 | 93,49 |
| P | 99,86 | 91,50 | 99,96 | 96,66 | 91,96 |
| PL | 99,82 | 88,27 | 99,99 | 99,77 | 91,29 |
| AVG | 99,90 | 95,83 | 99,99 | 99,77 | 94,67 |

The classification results of the two proposed models are depicted in the confusion matrix (figure 9). From the confusion matrix results, the proposed CNN-LSTM model has very good classification results in almost all MI classes (in lead II). The proposed CNN-LSTM model succeeded in classifying well (100%) in the IP, L, P, and PL classes, while the normal class had a value of 100%, which means there were no errors in the labeling. Meanwhile, in the proposed CNN-BILSTM model, in general the classes AL, I, IP, IPL, L and P are recognized well (100%), while the normal class has a value of 98.91% with an error of 1.09%.

a b

Fig. 9. a. Confusion matrix 10 MI class dan normal class di lead II, b. Confusion matrix 10 MI dan normal class di lead V4

## V. DISCUSSION

MI classification has been carried out in various studies. The fundamental difference lies in the classification algorithm used, the number of MI classes and the number of leads to compare the performance of the proposed models. Table 8 presents several studies that have been conducted and published using the current approach:

TABLE VIII. COMPARISON OF METHODS FOR DETECTION MI

| Ref | Year | Lead / Class | Classifier | Acc Rate |
|---|---|---|---|---|
| [28] | 2019 | Lead II / AMI, IMI and HC | LSTM | 99,91% |
| [29] | 2021 | 12 Lead ECG / Normal, MI and Non MI | CNN - BILSTM | 99,24% |
| [30] | 2021 | 12 Lead ECG/Normal & MI | CNN | 99,82% |
| [27] | 2023 | Lead V3, V4 and V6 / MI, Normal and Other | CNN – BILSTM | 93% |
| This work | 2023 | 15 Lead ECG / 10 MI class and normal class | CNN-LSTM & CNN-BILSTM | 98,80% & 99,90% |

Several studies related to MI classification using CNN and LSTM/BILSTM architectures have been carried out with different numbers of MI classes and leads. Zhang et al [28] used the LSTM architecture to classify AMI, IMI and HC classes in lead II of the public ECG Physiobank (PTB) database. The accuracy produced by this method is 99.91%. The study conducted by Dey et al. [29] to classify MI, Normal and Non MI classes for 12 lead ECG signals using CNN and bi LSTM models. The performance results of the proposed model are 99.246%. Meanwhile, Yadav et al. classifying MI and Normal classes with a CNN architecture model on 12-lead ECG signals with an accuracy of 99.82% [30]. Research conducted by Hasbullah et al. [27] proposed the CNN-BILSTM architecture on the 3 ECG signal leads of the PTB-XL public database. 93%. In our proposed research, we utilize 15 ECG signal leads in the PTB database. This study aims to create a simple model with two CNN architectures and LSTM / BILSTM to classify 10 MI classes and normal classes. Evaluation of the performance of the two CNN-LSTM/BILSTM models using multifaceted evaluation is needed to evaluate classification performance on imbalanced data. Performance evaluation can be derived with a performance matrix consisting of accuracy (Acc), sensitivity (Sens), specificity (Spec), precision (Pre) and F1-score [31].

## VI. CONCLUSION

In this study, two simple architectures were developed which focused on classifying 10 MI classes and normal classes using 15 ECG signal leads. The final result of this research is to propose a simple architecture of 9 layers CNN-LSTM and 10 layers CNN-BILSTM with 2 layers of

convolution, maxpolling, drouput, flatten, dense and 1 layer of LSTM and Bidirectional layer. After training for the two models, the test results for the two models showed performance on 15 leads with an average accuracy value of more than 98% for the two models. The CNN-LSTM model was able to produce the highest accuracy value in lead II of 99.93% for 10 MI classes and the normal class. Meanwhile, the CNN-BILSTM model produces the best average accuracy value for the 10 MI classes and the normal class of 99.90% in lead V4. The results of the overall performance evaluation of the two proposed models for classifying 10 MI classes and normal classes in 15-lead ECG signals have resulted in achieving accuracy, sensitivity, specificity, precision and f1-score above 94% for the CNN-LSTM model and above 91% for the CNN-BILSTM model. The best accuracy value in the CNN-LSTM model reached 99.95% in the posterolateral (PL) class, while in the CNN-BILSTM model the best accuracy value was 99.90% in the lateral (L) class. In terms of average accuracy for 15 lead ECGs, CNN-LSTM is a better model than CNN-BILSTM (98.80 vs. 98.62), but for all classes (MI and normal), CNN-BILSTM is better than CNN-LSTM (99.90 vs. 98.80). Compared to previous research, this research focuses on producing a simple architecture with a small number of layers with the aim of reducing computation time so that it is suitable for integration with medical devices. This research also focused on the classification of 10 MI classes and normal classes on 15-lead ECG signals. This causes the proposed CNN-LSTM/BILSTM model to be richer when compared with other studies that use 12-lead ECG signals.

## REFERENCES


[1] P. Xiong, S. M.-Y. Lee, and G. Chan, "Deep Learning for Detecting and Locating Myocardial Infarction by Electrocardiogram: A Literature Review," *Front Cardiovasc Med*, vol. 9, no. March, pp. 1–28, 2022, doi: 10.3389/fcvm.2022.860032.

[2] A. Nursalim, M. Suryaatmadja, and M. Panggabean, "Potential clinical application of novel cardiac biomarkers for acute myocardial infarction.," *Acta Med Indones*, vol. 45, no. 3, pp. 240–250, 2013.

[3] A. Darmawahyuni, S. Nurmaini, and Sukemi, "Deep Learning with Long Short-Term Memory for Enhancement Myocardial Infarction Classification," *Proceedings of the 2019 6th International Conference on Instrumentation, Control, and Automation, ICA 2019*, no. August 2019, pp. 19–23, 2019, doi: 10.1109/ICA.2019.8916683.

[4] K. Thygesen, J. S. Alpert, and H. D. White, "Universal Definition of Myocardial Infarction," *J Am Coll Cardiol*, vol. 50, no. 22, pp. 2173–2195, 2007, doi: 10.1016/j.jacc.2007.09.011.

[5] A. Strong, G. Sharma, C. Tu, A. Aminian, J. Rodriguez, and M. D. Kroh, "A Population-Based Study of Early Postoperative Outcomes in Patients Undergoing Bariatric Surgery with Congestive Heart Failure," *J Am Coll Surg*, vol. 225, no. 4, p. e55, 2017, doi: 10.1016/j.jamcollsurg.2017.07.666.

[6] P. Valensi, L. Lorgis, and Y. Cottin, "Prevalence, incidence, predictive factors and prognosis of silent myocardial infarction: A review of the literature," *Archives of Cardiovascular Diseases*, vol. 104, no. 3. pp. 178–188, Mar. 2011. doi: 10.1016/j.acvd.2010.11.013.

[7] C. Hainaut and W. Gade, "The emerging roles of BNP and accelerated cardiac protocols in emergency laboratory medicine.," *Clin Lab Sci*, vol. 16, no. 3, pp. 166–179, 2003.

[8] R. D. A. Ricardo, R. A. Bassani, and J. W. M. Bassani, "A simple laboratory method for teaching how electrocardiogram is generated," *IFMBE Proc*, vol. 25, no. 12, pp. 385–387, 2009, doi: 10.1007/978-3-642-03893-8_111.

[9] R. J. Perez, *Design of Medical Electronic Devices*, vol. 1999, no. December. Academic Press, 2002.

[10] P. J. Zimetbaum and M. E. Josephson, "Use of the Electrocardiogram in Acute Myocardial Infarction," *N Engl J Med*, vol. 348, pp. 933–940, 2003, doi: 10.1056/NEJMra022700.

[11] S. Nurmaini and U. Sriwijaya, "Cardiac Arrhythmias Classification Using Deep Neural Networks and Principle Component Analysis Algorithm," vol. 348, no. January, 2018.

[12] S. Banerjee, S. Member, and M. Mitra, "Application of Cross Wavelet Transform for ECG Pattern Analysis and Classification," no. February, 2014, doi: 10.1109/TIM.2013.2279001.

[13] S. Meek and F. Morris, "ABC of clinical electrocardiography Introduction. I-Leads, rate, rhythm, and cardiac axis."

[14] J. Tranchesi *et al.*, "The Vectorcardiogram in Dorsal or Posterior Myocardial Infarction*," Sao Paulo, 1961. doi: doi: 10.1016/0002-9149(61)90507-0.

[15] L. Hähnle, C. Viljoen, J. Hoevelmann, R. Gill, and A. Chin, "Posterior infarction: a STEMI easily missed," *Cardiovasc J Afr*, vol. 31, no. 6, pp. 51–54, Dec. 2020, doi: 10.5830/CVJA-2020-059.

[16] A. Gupta, E. A. Huerta, Z. Zhao, and I. Moussa, "Deep Learning for Cardiologist-level Myocardial Infarction Detection in Electrocardiograms," Dec. 2019, doi: 10.1007/978-3-030-64610-3_40.

[17] L. Fu, B. Lu, B. Nie, Z. Peng, H. Liu, and X. Pi, "Hybrid network with attention mechanism for detection and location of myocardial infarction based on 12-lead electrocardiogram signals," *Sensors (Switzerland)*, vol. 20, no. 4, Feb. 2020, doi: 10.3390/s20041020.

[18] A. H. Mirza, S. Nurmaini, and R. U. Partan, "Automatic Classification of 15 Leads ECG Signal of Myocardial Infarction Using One Dimension Convolutional Neural Network," *Applied Sciences (Switzerland)*, vol. 12, no. 11, Jun. 2022, doi: 10.3390/app12115603.

[19] E. Derya Übeyli, "Recurrent neural networks employing Lyapunov exponents for analysis of ECG signals," *Expert Syst Appl*, vol. 37, no. 2, pp. 1192–1199, Mar. 2010, doi: 10.1016/j.eswa.2009.06.022.

[20] Ralf-Dieter Bousseljot, "PTB Diagnostic ECG Database." [Online]. Available: https://physionet.org/content/ptbdb/1.0.0/

[21] S. Nurmaini *et al.*, "Robust detection of atrial fibrillation from short-term electrocardiogram using convolutional neural networks," *Future Generation Computer Systems*, vol. 113, pp. 304–317, 2020, doi: 10.1016/j.future.2020.07.021.

[22] Q. Qin, J. Li, L. Zhang, Y. Yue, and C. Liu, "Combining Low-dimensional Wavelet Features and Support Vector Machine for Arrhythmia Beat Classification," *Sci Rep*, vol. 7, no. 1, pp. 1–12, 2017, doi: 10.1038/s41598-017-06596-z.

[23] S. Nurmaini *et al.*, "An automated ECG beat classification system using deep neural networks with an unsupervised feature extraction technique," *Applied Sciences (Switzerland)*, vol. 9, no. 14, 2019, doi: 10.3390/app9142921.

[24] Y. Le Cun *et al.*, "Backpropagation applied to digit recognition," *Neural computation*, vol. 1, no. 4. pp. 541–551, 1989. [Online]. Available: https://www.ics.uci.edu/~welling/teaching/273ASpring09/lecun-89e.pdf

[25] U. R. Acharya, H. Fujita, S. L. Oh, Y. Hagiwara, J. H. Tan, and M. Adam, "Application of deep convolutional neural network for automated detection of myocardial infarction using ECG signals," *Inf Sci (N Y)*, vol. 415–416, pp. 190–198, 2017, doi: 10.1016/j.ins.2017.06.027.

[26] C. Chen, Z. Hua, R. Zhang, G. Liu, and W. Wen, "Automated arrhythmia classification based on a combination network of CNN and LSTM," *Biomed Signal Process Control*, vol. 57, p. 101819, 2020, doi: 10.1016/j.bspc.2019.101819.

[27] S. Hasbullah, M. S. Mohd Zahid, and S. Mandala, "Detection of Myocardial Infarction Using Hybrid Models of Convolutional Neural Network and Recurrent Neural Network," *BioMedInformatics*, vol. 3, no. 2, pp. 478–492, Jun. 2023, doi: 10.3390/biomedinformatics3020033.

[28] X. Zhang, R. Li, Q. Hu, B. Zhou, and Z. Wang, "A New automatic approach to distinguish myocardial infarction based on lstm," *2019 8th International Symposium on Next Generation Electronics, ISNE 2019*, pp. 1–3, 2019, doi: 10.1109/ISNE.2019.8896550.

[29] M. Dey, N. Omar, and M. A. Ullah, "Temporal Feature-Based Classification into Myocardial Infarction and Other CVDs Merging CNN and Bi-LSTM from ECG Signal," *IEEE Sens J*, vol. 21, no. 19, pp. 21688–21695, 2021, doi: 10.1109/JSEN.2021.3079241.

[30] S. S. Yadav, S. B. More, S. M. Jadhav, and S. R. Sutar, "Convolutional neural networks based diagnosis of myocardial infarction in electrocardiograms," *Proceedings - IEEE 2021 International Conference on Computing, Communication, and Intelligent Systems, ICCCIS 2021*, no. April, pp. 581–586, 2021, doi: 10.1109/ICCCIS51004.2021.9397193.

[31] M. Ohsaki, P. Wang, K. Matsuda, S. Katagiri, H. Watanabe, and A. Ralescu, "Confusion-matrix-based kernel logistic regression for imbalanced data classification," *IEEE Trans Knowl Data Eng*, vol. 29, no. 9, pp. 1806–1819, 2017, doi: 10.1109/TKDE.2017.2682249.